FITEE

A projected gradient based game theoretic approach for multi-user power control in cognitive radio network[*]

Yun-zheng TAO[‡1], Chun-yan WU[1], Yu-zhen HUANG[1,2], Ping ZHANG[1]

[1]State Key Laboratory of Networking and Switching Technology,

Beijing University of Posts and Telecommunications, Beijing 100876, China

[2]College of Communications Engineering, PLA University of Science and Technology, Nanjing 210007, China

E-mail: yunzhengtao@bupt.edu.cn; chunyanwuarkiro@163.com; yzh_huang@sina.com; pzhang@bupt.edu.cn

Abstract: The fifth generation (5G) networks have been envisioned to support the explosive growth of data demand caused by the increasing traditional high-rate mobile users and the expected rise of interconnections between human and things. To accommodate the ever-growing data traffic with scarce spectrum resources, cognitive radio (CR) is considered a promising technology to improve spectrum utilization. We study the power control problem for secondary users in an underlay CR network. Unlike most existing studies which simplify the problem by considering only a single primary user or channel, we investigate a more realistic scenario where multiple primary users share multiple channels with secondary users. We formulate the power control problem as a non-cooperative game with coupled constraints, where the Pareto optimality and achievable total throughput can be obtained by a Nash equilibrium (NE) solution. To achieve NE of the game, we first propose a projected gradient based dynamic model whose equilibrium points are equivalent to the NE of the original game, and then derive a centralized algorithm to solve the problem. Simulation results show that the convergence and effectiveness of our proposed solution, emphasizing the proposed algorithm, are competitive. Moreover, we demonstrate the robustness of our proposed solution as the network size increases.

Key words: Cognitive radio networks; Multi-user power control; Non-cooperative game; Nash equilibrium; Projected gradient

1 Introduction

Spectrum scarcity has been considered a primary problem in the fifth generation (5G) networks when trying to meet the data requirement of new wireless services, such as the Internet of Things (IoT), which comprises billions of devices and the

comprehensive applications of augmented/virtual reality (AR/VR). While developing unlicensed spectrum is a possible solution to the problem, recent spectrum utilization measurements reveal that the licensed spectra are actually underused. The limited spectrum resources are wasted by the static and rigid spectrum management regimes which are currently in use. Therefore, it is important to consider possible improvements in spectrum utilization by employing the latest technologies. Cognitive radio (CR) technology, which is able to facilitate more efficient spectrum utilization, is considered a promising technology to solve the contradiction between ceaseless demands for spectrum and finite spectrum

resources (Han et al., 2012). In CR networks, the co-channel interference (CCI) in radio transmission and the interference temperature regulation imposed by primary users (PUs) make power control a significant issue. For spectrum sharing, secondary users (SUs) can access the licensed spectrum by two methods: overlay or underlay mode. In the latter, SUs are allowed to interfere with PUs below a predetermined level, called the 'interference temperature' (Le and Hossain, 2008). Therefore, PUs can consider the power of SUs noises, which can be quantized and judged. As long as the interference is less than the threshold predefined by PUs, SUs are allowed to access the spectrum. Thus, it is not trivial to set the optimal tolerable interference level for PUs. Existing studies have proposed all kinds of techniques to address related problems, including the detection of leaked oscillator power (Wild and Ramchandran, 2005), the interference temperature model (Kolodzy, 2006), and sensor-aided spectrum sensing (Mercier et al., 2008).

In CR power control related research, a single PU or a single-channel scenario has been investigated broadly when formulating the problem. Wang et al. (2013) and Yang et al. (2015) considered only a single PU. Yang et al. (2015) and Zhou et al. (2012) investigated a single-channel model. Yang et al. (2015) proposed a fast and low-complexity adaptive power control iterative algorithm; however, they did not prove that the obtained solution conforms to the interference constraints of PUs. In Zhou et al. (2012), a robust distributed power control algorithm, which does not apply a pricing mechanism, was designed through reinforcement learning. It is considered to be the first algorithm to solve the incomplete-information power control game in CR networks. Bedeer et al. (2014) took multiple PUs and channels into consideration, exploiting a multi-objective optimization approach to investigate the optimal link adaptation problem in orthogonal frequency-division multiplexing (OFDM) based CR systems. It is formulated as a problem that jointly maximizes the system's throughput and minimizes its transmission power, subject to the interference constraints for PUs, the quality of service (QoS) requirements of SUs in terms of the maximum bit error rate, transmission power budget, and maximum number of allocated bits per subcarrier. Although Bedeer et al. (2014) thoughtfully took into account errors due to

imperfect sensing of PUs' frequency bands, they considered only the single-SU situation.

Game theory provides the ideal framework for designing efficient and robust distributed algorithms in wireless communication networks, especially in CR networks. All kinds of game models have been proposed to solve power control problems in CR networks, including repeated, myopic, S-modular, and potential games. These games were introduced and their convergence conditions were demonstrated by Neel et al. (2004). Wu and Tsang (2008) derived a distributed algorithm based on a layered structure similar to the Stackelberg game, in which, with the help of monitoring sensors deployed in the vicinity of PUs, SUs' power strategies are able to converge to the unique Nash equilibrium (NE), subject to constraints on both SUs and PUs. However, this algorithm requires a relatively high signal-to-interference-plus-noise ratio (SINR) of every SU and fails to prove the convergence of the algorithm. In most existing work, SUs need to share interference channel information and power strategies to implement the game with a pricing mechanism that requires frequent exchange of information. Based on CR networks with multiple PUs and multiple channels, Lin et al. (2010) proposed a distributed power control algorithm whose objective is to maximize the secondary capacity; however, the solution proposed in this study incurs a significant information exchange overhead, requiring increased resulting time and complexity.

Motivated by the limitations in these existing studies, we consider a more realistic scenario in CR networks where multiple PUs share multiple channels with SUs. We model the power control problem as a non-cooperative game with coupled constraints. Then we propose a centralized power control algorithm based on projected gradient that can achieve an NE of the game. The main contributions of this paper are summarized as follows:

1. Multi-PU and multichannel power control game formulation: Unlike many existing studies which considered one single PU or channel, we investigate the power control problem in multi-PU and multichannel CR networks, which is a much more complicated problem. Hence, we consider the distributed alternative and formulate the distributed power control problem as a non-cooperative game with coupled constraints. The existence of NE for

this game is demonstrated.

2. A projected gradient based dynamic model: To find the NE of the power control game, we propose a projected gradient based dynamic model whose equilibrium points are equivalent to an NE of the original game. Therefore, pursuing NE of the original game is converted to solving equilibrium points of the dynamic model. This procedure involves each SU's power strategies and some other information, and determines the model as a centralized power control scheme.

3. Centralized projected gradient based power control algorithm design: To solve the equilibrium points of the proposed model, we next devise a centralized power control algorithm based on projected gradient, which achieves an NE of the non-cooperative power control game. The convergence of the proposed algorithm is illustrated by simulation results, and the effectiveness is shown by comparison with another algorithm. Furthermore, the robustness of the proposed algorithm is demonstrated with the increase of the network size.

2 System description

In this section, we describe the system model and then present the game formulation.

2.1 System model

The proposed system model is based on Wu and Tsang (2008). It is depicted in the simplified abstract diagram (Fig. 1), where there are M PUs and N SUs. Each SU is a transceiver pair and is denoted as (SU_i-Tx, SU_i-Rx) ($1 \leq i \leq N$). In the vicinity of each PU, there is a monitoring sensor ($\text{MS}_m, 1 \leq m \leq M$), which is equipped by a PU to monitor the interference level from each SU to PU_m over each channel. These sensors are omitted in the diagram for clarity. We consider the uplink transmission of SUs, where the blue solid lines represent data transmission links between the SU transceiver pairs, and the blue chain lines and red dashed lines denote interference from SU-Tx to SU-Rx and PU, respectively. Note that we focus on exploring the power control game in a wireless interference model, and thus some physical layer channel access schemes (e.g., code-division multiple access (CDMA)) can be adopted to allow SUs to share the same spectrum resource simultaneously and efficiently. The available spectrum is assumed to

be divided into K sub-channels, each with an equal bandwidth W. Let $\boldsymbol{g}_{ij} = \left(g_{ji}^1, g_{ji}^2, \cdots, g_{ji}^K\right)$ be the link power gain vector from SU_j-Tx to SU_i-Rx over K channels and $\boldsymbol{h}_{im} = \left(h_{im}^1, h_{im}^2, \cdots, h_{im}^K\right)$ be the link power gain vector from SU_i-Tx to PU_m over K channels.
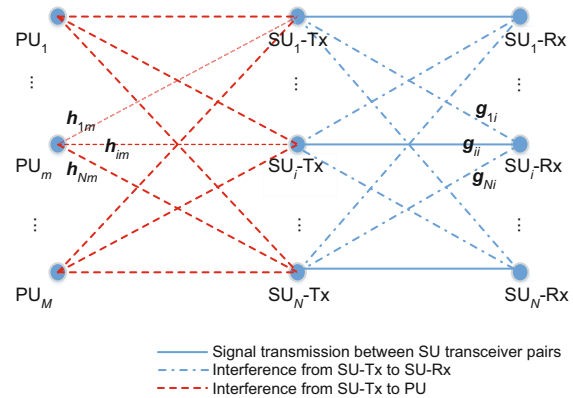
Fig. 1 System model with M PUs and N secondary transceiver pairs
PU: primary user; SU-Tx: secondary user transmitter; SU-Rx: secondary user receiver. $i, j = 1, 2, \cdots, N$; $m = 1, 2, \cdots, M$. References to color refer to the online version of this figure

We assume that the spectrum sharing mode in this study is underlay, where SUs are allowed to access the licensed spectrum as long as the interference power does not exceed a predefined threshold at PUs. We employ the interference temperature model (Kolodzy, 2006) as a metric for interference incurred by PUs. By designating the interference temperature threshold, the power controller will govern the operation of the CR system to ensure that PUs will not be affected adversely. The interference power threshold imposed by the mth PU can be calculated as $\kappa T_m K W$, where κ is the Boltzmann constant and T_m is its interference temperature threshold.

2.2 Game formulation

Based on the system model presented in Section 2.1, we consider a power control strategy $\boldsymbol{p}_i = \left(p_i^1, p_i^2, \cdots, p_i^K\right)$ ($1 \leq i \leq N$) for each SU. The goal of each strategy is to maximize the channel capacity for the specific SU when satisfying the interference temperature regulation and its transmission power budget. The strategic game can be defined as follows:

Definition 1   The non-cooperative power control game in strategic form is a triplet $G = \{\mathcal{N}, S,$

$(u_i)_{i \in \mathcal{N}}\}$, where $\mathcal{N}$ is a finite set of players, i.e., $\mathcal{N} = \{1, 2, \cdots, N\}$, $S = \boldsymbol{p}_1 \cdot \boldsymbol{p}_2 \cdot \ldots \cdot \boldsymbol{p}_i \cdot \ldots \cdot \boldsymbol{p}_N$ is the set of pure strategies for players, and u_i is the utility function for player i.

Note that the players are assumed to be SUs, and the pure strategy space is expressed as

$$S = \Big\{ \boldsymbol{p} = (\boldsymbol{p}_1, \boldsymbol{p}_2, \cdots, \boldsymbol{p}_N)^{\mathrm{T}} \in \times_{i=1,2,\cdots,N} \Omega_i |$$
$$\sum_{i=1}^{N} \sum_{k=1}^{K} p_i^k h_{im}^k \leq \kappa T_m KW, \ m = 1, 2, \cdots, M \Big\}, \quad (1)$$

where Ω_i denotes the set of transmit power for SU_i-Tx, given by

$$\Omega_i = \Big\{ (p_i^1, p_i^2, \cdots, p_i^K)^{\mathrm{T}} \in \mathbb{R}^K |$$
$$p_i^k \geq 0, \ \sum_{k=1}^{K} p_i^k \leq p_i^{\max}, \ k = 1, 2, \cdots, K \Big\}, \quad (2)$$

where $p_i^{\max}$ denotes the power budget of SU_i-Tx. Then the SU_i-Tx strategy space can be denoted as

$$S_i(\boldsymbol{p}_{-i}) = \Big\{ \boldsymbol{p}_i \in \Omega_i | \sum_{i=1}^{N} \sum_{k=1}^{K} p_i^k h_{im}^k \leq \kappa T_m KW,$$
$$m = 1, 2, \cdots, M \Big\}. \quad (3)$$

It is easily observed that strategy sets are non-orthogonal, meaning that G is a coupled constraint game. In this game, the utility function is the throughput of each SU, represented by channel capacity as

$$u_i = \sum_{k=1}^{K} u_i^k = W \sum_{k=1}^{K} \log_2 \left(1 + \frac{p_i^k g_{ii}^k}{\sum_{\substack{j=1 \\ j \neq i}}^{N} p_j^k g_{ji}^k + I_i^k} \right), \quad (4)$$

where I_i^k is the background noise power of SU_i-Rx over channel k. Note that the interference from PUs to SU_i over channel k is included in I_i^k.

Based on this non-cooperative game, we then define NE to deal with pure strategies.

Definition 2 A pure-strategy NE of the non-cooperative power control game $G = \{\mathcal{N}, S, (u_i)_{i \in \mathcal{N}}\}$ is a strategy profile $\boldsymbol{p}^* \in S$ such that

$$u_i(\boldsymbol{p}_{-i}^*, \boldsymbol{p}_i^*) \geq u_i(\boldsymbol{p}_{-i}^*, \boldsymbol{p}_i), \ \forall \boldsymbol{p}_i \in S_i, \forall i \in \mathcal{N}. \quad (5)$$

In other words, given that other SUs' strategies remain fixed, if no SU has an incentive to

deviate unilaterally to another transmit power strategy, the strategy is a pure-strategy NE, which is $\boldsymbol{p}^* = (\boldsymbol{p}_1, \boldsymbol{p}_2, \cdots, \boldsymbol{p}_N)$.

Then we investigate the existence of NE for G. The result is stated in Theorem 1.

Theorem 1 There exists at least one pure-strategy NE for the coupled constraint game G over the strategy space S.

Proof For a non-cooperative game with coupled constraints, Arrow et al. (1961) gave sufficient conditions for the existence of an NE. In our power control game, they can be translated as: joint strategy space S is a nonempty closed bounded convex subset on $\mathbb{R}^N$, and for each $i \in \mathcal{N}$, its utility function $u_i(\boldsymbol{p}_{-i}, \boldsymbol{p}_i)$ is continuous on S and concave in $\boldsymbol{p}_i$.

Because S is a nonempty closed bounded set and is also the intersection of convex set $\times_{i=1,2,\cdots,N} \Omega_i$ and half-space $\sum_{i=1}^{N} \sum_{k=1}^{K} p_i^k h_{im}^k \leq \kappa T_m KW$ ($m = 1, 2, \cdots, M$), it is a nonempty closed bounded convex subset on $\mathbb{R}^N$.

Obviously, utility function $u_i(\boldsymbol{p}_{-i}, \boldsymbol{p}_i)$ is continuous on S. Its first partial derivative with respect to $\boldsymbol{p}_i$ is

$$\frac{\partial u_i}{\partial \boldsymbol{p}_i} = \frac{W}{\ln 2}$$
$$\cdot \left(\frac{g_{ii}^1}{\sum\limits_{j=1}^{N} p_j^1 g_{ji}^1 + I_i^1}, \frac{g_{ii}^2}{\sum\limits_{j=1}^{N} p_j^2 g_{ji}^2 + I_i^2}, \cdots, \frac{g_{ii}^K}{\sum\limits_{j=1}^{N} p_j^K g_{ji}^K + I_i^K} \right)^{\mathrm{T}}, \quad (6)$$

and its second partial derivative with respect to $\boldsymbol{p}_i$ is given by

$$\frac{\partial^2 u_i}{\partial \boldsymbol{p}_i^2} = \frac{W}{\ln 2} \cdot \mathrm{diag} \left(\frac{-(g_{ii}^1)^2}{\left(\sum\limits_{j=1}^{N} p_j^1 g_{ji}^1 + I_i^1 \right)^2}, \right.$$
$$\left. \frac{-(g_{ii}^2)^2}{\left(\sum\limits_{j=1}^{N} p_j^2 g_{ji}^2 + I_i^2 \right)^2}, \cdots, \frac{-(g_{ii}^K)^2}{\left(\sum\limits_{j=1}^{N} p_j^K g_{ji}^K + I_i^K \right)^2} \right). \quad (7)$$

It can be observed easily that Eq. (7) is a negative definite matrix, and thus $u_i(\boldsymbol{p}_{-i}, \boldsymbol{p}_i)$ is concave in $\boldsymbol{p}_i$.

Therefore, G satisfies the above sufficient conditions, and there exists at least one NE for G.

3 Property analysis of the game

3.1 A dynamic model based on projected gradient

The NE solution to G is a fixed point. It is challenging to acquire the closed-form expression of the solution. Therefore, we exploit certain mathematical programming computational methods instead. First, we use a continuous-time dynamic adjustment process of a non-cooperative power control game proposed by Rosen (1965), where each player changes its own power strategy, so that the joint power strategies remain in S, and its own utility function would increase, assuming that all other players hold their current strategies. In other words, each player changes its power strategy at a rate proportional to the gradient of its utility function with respect to its strategy, subject to the constraints.

For analytical convenience, the strategy space is rewritten as the following matrix-form inequality:

$$S = \left\{ \boldsymbol{p} = (\boldsymbol{p}_1; \boldsymbol{p}_2; \cdots ; \boldsymbol{p}_N) \in \mathbb{R}^{K \times N} \mid \boldsymbol{s}(\boldsymbol{p}) \geq 0 \right\}, \quad (8)$$

where vector $\boldsymbol{s}(\boldsymbol{p}) \in \mathbb{R}^{N(K+1)+M}$ corresponds to $(N(K+1)+M)$ constraints of the strategy space. Specifically, we have

$$\boldsymbol{s}(\boldsymbol{p}) = \boldsymbol{A}\boldsymbol{p} - \boldsymbol{b}, \quad (9)$$

where $\boldsymbol{A}$ and $\boldsymbol{b}$ are given by Eq. (10) shown on the bottom of this page. For the sake of easy

representation, let $C_m = \kappa T_m K W$ $(1 \leq m \leq M)$. The dynamic system under consideration can be characterized by the following differential:

$$\frac{\mathrm{d}\boldsymbol{p}}{\mathrm{d}t} = \left[\frac{\partial u_i}{\partial \boldsymbol{p}_i}\right]_{(i)} + \sum_{z=1}^{N(K+1)+M} \lambda_z \frac{\partial s_z(\boldsymbol{p})}{\partial \boldsymbol{p}}. \quad (11)$$

By Eq. (9), we have

$$\frac{\partial s_z(\boldsymbol{p})}{\partial \boldsymbol{p}} = \boldsymbol{A}_z^{\mathrm{T}}, \ 1 \leq z \leq N(K+1) + M, \quad (12)$$

where $\boldsymbol{A}_z^{\mathrm{T}}$ is the transpose of the zth vector of matrix $\boldsymbol{A}$, and set λ lying in a bounded subset of the positive orthant of $\mathbb{R}^{N(K+1)+M}$ is selected appropriately to ensure that set λ starts with any $\boldsymbol{p} \in S$ and the solution of G remains in S. This will be discussed later in this section. Note that λ is denoted by

$$\lambda = \left\{ \arg\min_{\substack{\lambda_z \geq 0, s_z(\boldsymbol{p}) \leq 0 \\ \lambda_z = 0, s_z(\boldsymbol{p}) > 0}} ||f(\boldsymbol{p}, \lambda)|| \, \Big| \lambda \in \mathbb{R}^{N(K+1)+M} \right\}, \quad (13)$$

where $f(\boldsymbol{p}, \lambda)$ is the projection of the pseudo-gradient of the individual utility function with respect to its corresponding power strategy on the manifold formed by the active constraints at $\boldsymbol{p}$.

According to the lemma in Rosen (1965), we can acquire the closed-form expression of λ, where the vector consisting of nonzero elements in λ is

$$\overline{\lambda} = -\left(\overline{\boldsymbol{A}}\overline{\boldsymbol{A}}^{\mathrm{T}}\right)^{-1}\overline{\boldsymbol{A}}\left[\frac{\partial u_i}{\partial \boldsymbol{p}_i}\right]_{(i)}, \quad (14)$$

$$\boldsymbol{A} = \begin{pmatrix} 1 & & & & & & & & & & & \\ & 1 & & & & & & & & & & \\ & & \ddots & & & & & & & & & \\ & & & 1 & & & & & & & & \\ -1 & -1 & \cdots & -1 & & & & & & & & \\ & & & & 1 & & & & & & & \\ & & & & & \ddots & & & & & & \\ & & & & & & 1 & & & & & \\ & & & & & & & 1 & & & & \\ & & & & & & & & \ddots & & & \\ & & & & & & & & & 1 & & \\ & & & & & & & -1 & -1 & \cdots & -1 & \\ -h_{11}^1 & -h_{11}^2 & \cdots & -h_{11}^K & -h_{21}^{K-1} & \cdots & -h_{N1}^1 & -h_{N1}^2 & \cdots & -h_{N1}^K \\ -h_{12}^1 & -h_{12}^2 & \cdots & -h_{12}^K & -h_{22}^{K-1} & \cdots & -h_{N2}^1 & -h_{N2}^2 & \cdots & -h_{N2}^K \\ \vdots & \vdots & & \vdots & \vdots & & \vdots & \vdots & & \vdots \\ -h_{1M}^1 & -h_{1M}^2 & \cdots & -h_{1M}^K & -h_{2M}^{K-1} & \cdots & -h_{NM}^1 & -h_{NM}^2 & \cdots & -h_{NM}^K \end{pmatrix}, \quad \boldsymbol{b} = \begin{pmatrix} 0 \\ 0 \\ \vdots \\ 0 \\ -p_1^{\max} \\ 0 \\ 0 \\ \vdots \\ 0 \\ -p_N^{\max} \\ C_1 \\ C_2 \\ \vdots \\ C_M \end{pmatrix}. \quad (10)$$

where $\overline{A}$ consists of every A_z that satisfies $A_z p - b_z \leq 0$. Then let the right-hand side of Eq. (11) be

$$\left[\frac{\partial u_i}{\partial \boldsymbol{p}_i}\right]_{(i)} + \sum_{z=1}^{N(K+1)+M} \lambda_z \frac{\partial s_z(\boldsymbol{p})}{\partial \boldsymbol{p}} = f(\boldsymbol{p}, \lambda). \quad (15)$$

Now we introduce a useful definition of a dynamic system that will be used to prove Theorem 2, i.e., the equilibrium point (Rosen, 1965).

Definition 3　We call $\overline{\boldsymbol{p}}$ an 'equilibrium point', if

$$f(\overline{\boldsymbol{p}}, \lambda) = 0. \quad (16)$$

3.2 Equilibrium points of the dynamic system

In Theorem 2, we exploit Karush-Kuhn-Tucker (KKT) conditions at NE and the specialty of the equilibrium point of the above dynamic system. The desired results enable us to find the NE for the considered game by updating the power strategies on the basis of the dynamic system.

Theorem 2　The equilibrium points of the dynamic system defined by Eqs. (11) and (13) are equivalent to the NE of G.

Proof　According to the sufficiency of KKT conditions (Rosen, 1965) at NE of G, if $\exists (\boldsymbol{p}^*, \boldsymbol{\alpha}^*)$ that satisfies conditions (17)–(19), then $(\boldsymbol{p}^*, \boldsymbol{\alpha}^*)$ is the NE of game G.

$$\boldsymbol{s}(\boldsymbol{p}^*) \geq 0, \quad (17)$$

$$\exists \boldsymbol{\alpha}^* \in \mathbb{R}^{N(K+1)+M}, \, \boldsymbol{\alpha}^* \geq 0 \quad (18)$$

$$\text{s.t. } (\boldsymbol{\alpha}^*)^{\mathrm{T}} \boldsymbol{s}(\boldsymbol{p}^*) = 0,$$

$$u_i(\boldsymbol{p}^*_{-i}, \boldsymbol{p}^*_i) \geq u_i(\boldsymbol{p}^*_{-i}, \boldsymbol{p}_{-i}) + (\boldsymbol{\alpha}^*)^{\mathrm{T}} \boldsymbol{s}(\boldsymbol{p}^*_{-i}, \boldsymbol{p}_{-i}),$$

$$i = 1, 2, \cdots, N. \quad (19)$$

Because both $u_i(\boldsymbol{p})$ and $s_z(\boldsymbol{p})$ are differentiable concave functions, inequality (19) is equivalent to

$$\left[\frac{\partial u_i}{\partial \boldsymbol{p}_i}\right]_{(i)}\bigg|_{\boldsymbol{p}=\boldsymbol{p}^*} + \sum_{z=1}^{N(K+1)+M} \boldsymbol{\alpha}_z^* \frac{\partial \boldsymbol{s}_z(\boldsymbol{p}^*)}{\partial \boldsymbol{p}} = 0. \quad (20)$$

Although the equilibrium points of the dynamic model defined by Eqs. (11) and (13) also satisfy conditions (17)–(19), condition (17) is satisfied because there is a conclusion that starting with any point $\boldsymbol{p} \in S$, a continuous solution $\boldsymbol{p}(t)$ to the dynamic model exists, such that $\boldsymbol{p}(t)$ remains in S for all $t > 0$. The proof is similar to that in Rosen (1965); however, we omit it due to space limitations. Second, Eq. (13) is equivalent to constraint (18). Finally,

Eq. (16) is equivalent to Eq. (20) by definition of the equilibrium point.

Therefore, it is shown that the equilibrium points of the dynamic system are equivalent to the NE of G.

Though the continuous-time dynamic system is desired for finding the NE of the original game, it is not suitable for computational calculation. Therefore, the following discrete-time system, as an approximation of the continuous-time dynamic system, is considered to derive NE:

$$\boldsymbol{p}(n + 1) = \boldsymbol{p}(n) + \rho(n) f(\boldsymbol{p}(n), \lambda(n)), \quad (21)$$

$$\lambda(n) = \left\{ \lambda = \arg\min_{\substack{\lambda_z \geq 0, s_z(n) \leq 0 \\ \lambda_z = 0, s_z(n) > 0}} ||f(\boldsymbol{p}(n), \lambda)|| \, \bigg| \lambda \in \mathbb{R}^{N(K+1)+M} \right\}, \quad (22)$$

where n is the discrete-time variable and $\rho(n)$ is the step length.

With this discrete-time system, we can acquire the NE solution by a sequence of iteration transmission power vectors of all SUs. We are inclined to conclude that the iterative rule (Eq. (21)) and the selection of the step length (Eq. (22)) are similar to their counterparts in the general gradient projection method (Rosen, 1960), which is effective in solving constrained maximization. The only practical difference between the two methods is that in the latter case we choose the step length to give a maximum of the objective function along the chosen ray, whereas for the equilibrium point problem, we choose the step length to minimize the norm of f.

4 Centralized power control algorithm based on projected gradient design

4.1 A centralized gradient projection power control algorithm

In this subsection, we propose a centralized gradient projection (CGP) power control algorithm, presented in Algorithm 1.

Algorithm 1　Centralized gradient projection (CGP) power control algorithm

---

Input: g_{ji}^k, h_{im}^k, n_i^k, $p_i^{\max}$, and T_m ($i, j = 1, 2, \cdots, N$ and $m = 1, 2, \cdots, M$).
Output: $\boldsymbol{p}^*$.
Initialize: set $\boldsymbol{p}(1) \in S$, $\varepsilon > 0$, $n = 1$, and conti $= 1$.
1: **while** conti **do**

2:    Divide constraints by their activity, where $\boldsymbol{A}$ and $\boldsymbol{b}$ are divided as $(\boldsymbol{A}_1; \boldsymbol{A}_2)$ and $(\boldsymbol{b}_1; \boldsymbol{b}_2)$, respectively, such that $\boldsymbol{A}_1\boldsymbol{p}(n) \le \boldsymbol{b}_1$ and $\boldsymbol{A}_2\boldsymbol{p}(n) > \boldsymbol{b}_2$;

3:    Compute $\left[\frac{\partial u_i}{\partial \boldsymbol{p}_i}\right]_{(i)}\Big|_{\boldsymbol{p}=\boldsymbol{p}(n)}$;

4:    **while** 1 **do**
      // Compute projection matrix $\boldsymbol{P}$:

5:      **if** $\boldsymbol{A}_1$ is empty **then**

6:        Let $\boldsymbol{P} = \boldsymbol{E}_{NK}$;

7:      **else**

8:        Let $\boldsymbol{P} = \boldsymbol{E}_{NK} - \boldsymbol{A}_1{}^{\mathrm{T}}(\boldsymbol{A}_1\boldsymbol{A}_1{}^{\mathrm{T}})^{-1}\boldsymbol{A}_1$;

9:      **end if**
        // Seek the feasible searching direction $\boldsymbol{d}(n)$ for
        // the equilibrium point:

10:     Let $\boldsymbol{d}(n) = \boldsymbol{P}\left[\frac{\partial u_i}{\partial \boldsymbol{p}_i}\right]_{(i)}\Big|_{\boldsymbol{p}=\boldsymbol{p}(n)}$;

11:     **if** $\|\boldsymbol{d}(n)\| < \varepsilon$ **then**

12:       **if** $\boldsymbol{A}_1$ is empty **then**

13:         Output $\boldsymbol{p}^* = \boldsymbol{p}(n)$, conti $= 0$;

14:         **break;**

15:       **else**

16:         $\boldsymbol{w} = (\boldsymbol{A}_1\boldsymbol{A}_1{}^{\mathrm{T}})^{-1}\boldsymbol{A}_1\left[\frac{\partial u_i}{\partial \boldsymbol{p}_i}\right]_{(i)}\Big|_{\boldsymbol{p}=\boldsymbol{p}(n)}$;

17:         **if** $\boldsymbol{w} \le \boldsymbol{0}$ **then**

18:           Output $\boldsymbol{p}^* = \boldsymbol{p}(n)$, conti $= 0$;

19:           **break;**

20:         **else**

21:           Choose the maximum positive component of $\boldsymbol{w}$, getting rid of its corresponding row vector in $\boldsymbol{A}_1$;

22:         **end if**

23:       **end if**

24:     **else**

25:       **break;**

26:     **end if**

27:   **end while**

28:   Select step length $\rho(n)$ by solving constraint minimization:

$$\min_{\rho(n)} \left\| \boldsymbol{P}\left[\frac{\partial u_i}{\partial \boldsymbol{p}_i}\right]_{(i)}\Big|_{\boldsymbol{p}=\boldsymbol{p}(n)+\rho(n)\boldsymbol{d}(n)} \right\|$$
$$\text{s.t. } 0 \le \rho(n) \le \rho^{\max},$$

where $\rho^{\max}$ is determined by

$$\rho^{\max} = \begin{cases} \infty, & \mathbf{dd} \ge \boldsymbol{0}, \\ \min\left(\frac{\mathbf{bb}(j)}{\mathbf{dd}(j)} \mid \mathbf{dd}(j) < 0\right), & \text{otherwise,} \end{cases}$$

where $\mathbf{bb} = \boldsymbol{b_2} - \boldsymbol{A_2}\boldsymbol{p}(n)$ and $\mathbf{dd} = \boldsymbol{A_2}\boldsymbol{d}(n)$;

29:   **if** $\|\rho(n)\boldsymbol{d}(n)\| < \varepsilon$ **then**

30:     Output $\boldsymbol{p}^* = \boldsymbol{p}(n)$;

31:     **break;**

32:   **else**

33:     $\boldsymbol{p}(n+1) = \boldsymbol{p}(n) + \rho(n)\boldsymbol{d}(n), \ n = n+1$;

34:    **end if**
35: **end while**

Remark 1   CGP needs to be implemented with complete information, including the channel gain of channels between the SU transmitters and receivers and PU receivers, respectively. Those also required are the background noise power of SU receivers, the maximum transmit power budget of every SU, the interference temperature threshold of every PU, and the power allocation strategy of every SU during every stage. CGP requires a deep collaboration among SUs. It cannot achieve distributed implementation by individual SUs. Therefore, a central control node or a similar one is required in our algorithm.

Remark 2   Assume that the channel state is quasi-static during the procedure. Therefore, the proposed algorithm focuses on power control in slow time-varying environments.

4.2 Convergence analysis

Convergence has a critical relation with the accuracy and reliability of an algorithm. Accordingly, in this subsection, the convergence of our proposed algorithm is investigated. We obtain the following result using a method similar to the proof in Rosen (1965):

Theorem 3   A step length $\rho(n)$ can be chosen so that starting with any $\boldsymbol{p} \in S$, the dynamic system defined by Eqs. (21) and (22) converges to the NE of G.

Proof   For a fixed $\lambda(n)$, by the Lagrange mean value theorem, there exists a $\boldsymbol{p}_{\boldsymbol{\xi}_N}$ between $\boldsymbol{p}(n)$ and $\boldsymbol{p}(n+1)$, such that

$$\begin{aligned} f(\boldsymbol{p}(n+1), \lambda(n)) &= f(\boldsymbol{p}(n), \lambda(n)) \\ &+ F(\boldsymbol{p}_{\boldsymbol{\xi}_N})(\boldsymbol{p}(n+1) - \boldsymbol{p}(n)), \end{aligned} \quad (23)$$

where $F(\boldsymbol{p})$ is the Jacobian of $f(\boldsymbol{p}, \lambda)$ with respect to $\boldsymbol{p}$. Putting Eq. (15) into $f(\boldsymbol{p}, \lambda)$, we have

$$\begin{aligned} F(\boldsymbol{p}) &= \left(\frac{\partial f}{\partial \boldsymbol{p}_1{}^{\mathrm{T}}}, \frac{\partial f}{\partial \boldsymbol{p}_2{}^{\mathrm{T}}}, \cdots, \frac{\partial f}{\partial \boldsymbol{p}_N{}^{\mathrm{T}}} \right) \\ &= \boldsymbol{P} \begin{pmatrix} \dfrac{\partial^2 u_1}{\partial \boldsymbol{p}_1^2} & \dfrac{\partial^2 u_1}{\partial \boldsymbol{p}_1 \partial \boldsymbol{p}_2} & \cdots & \dfrac{\partial^2 u_1}{\partial \boldsymbol{p}_1 \partial \boldsymbol{p}_N} \\ \dfrac{\partial^2 u_2}{\partial \boldsymbol{p}_2 \partial \boldsymbol{p}_1} & \dfrac{\partial^2 u_2}{\partial \boldsymbol{p}_2 \partial \boldsymbol{p}_2} & \cdots & \dfrac{\partial^2 u_2}{\partial \boldsymbol{p}_2 \partial \boldsymbol{p}_N} \\ \vdots & \vdots & & \vdots \\ \dfrac{\partial^2 u_N}{\partial \boldsymbol{p}_N \partial \boldsymbol{p}_1} & \dfrac{\partial^2 u_N}{\partial \boldsymbol{p}_N \partial \boldsymbol{p}_2} & \cdots & \dfrac{\partial^2 u_N}{\partial \boldsymbol{p}_N^2} \end{pmatrix}, \end{aligned} \quad (24)$$

where $\boldsymbol{P}$ is the projection matrix introduced in Algorithm 1. Substituting Eq. (21) into Eq. (23), we have

$$
\begin{aligned}
&f(\boldsymbol{p}(n+1),\lambda(n))\\
&=(\boldsymbol{E}_{NK}+\rho(n)F(\boldsymbol{p}_{\boldsymbol{\xi}_N}))f(\boldsymbol{p}(n),\lambda(n)),
\end{aligned} \tag{25}
$$

where $\boldsymbol{E}_{NK}$ is the identity matrix of $N \times K$. Then

$$
\begin{aligned}
||f(\boldsymbol{p}(n+1),\lambda(n))||^2 &= ||f(\boldsymbol{p}(n),\lambda(n))||^2\\
&+ \rho(n)\big(\rho(n)||F(\boldsymbol{p}_{\boldsymbol{\xi}_N})f(\boldsymbol{p}(n),\lambda(n))||^2\\
&+ 2f^{\mathrm{T}}(\boldsymbol{p}(n),\lambda(n))F(\boldsymbol{p}_{\boldsymbol{\xi}_N})f(\boldsymbol{p}(n),\lambda(n))\big).
\end{aligned} \tag{26}
$$

To minimize $||f(\boldsymbol{p}(n+1),\lambda(n))||^2$, $\rho(n)$ is selected by

$$
\rho(n) = -\frac{f^{\mathrm{T}}(\boldsymbol{p}(n),\lambda(n))F(\boldsymbol{p}_{\boldsymbol{\xi}_N})f(\boldsymbol{p}(n),\lambda(n))}{||F(\boldsymbol{p}_{\boldsymbol{\xi}_N})f(\boldsymbol{p}(n),\lambda(n))||^2}. \tag{27}
$$

Thus,

$$
\begin{aligned}
||f(\boldsymbol{p}(n+1),\lambda(n))||^2 &= ||f(\boldsymbol{p}(n),\lambda(n))||^2\\
&- \frac{\big(f^{\mathrm{T}}(\boldsymbol{p}(n),\lambda(n))F(\boldsymbol{p}_{\boldsymbol{\xi}_N})f(\boldsymbol{p}(n),\lambda(n))\big)^2}{||F(\boldsymbol{p}_{\boldsymbol{\xi}_N})f(\boldsymbol{p}(n),\lambda(n))||^2}.
\end{aligned} \tag{28}
$$

Obviously,

$$
||f(\boldsymbol{p}(n+1),\lambda(n))||^2 < ||f(\boldsymbol{p}(n),\lambda(n))||^2. \tag{29}
$$

Because $\lambda(n+1)$ is selected to minimize $||f(\boldsymbol{p}(n+1),\lambda(n+1))||^2$, we have

$$
\begin{aligned}
&||f(\boldsymbol{p}(n+1),\lambda(n+1))||^2\\
&\leq ||f(\boldsymbol{p}(n+1),\lambda(n))||^2 < ||f(\boldsymbol{p}(n),\lambda(n))||^2.
\end{aligned} \tag{30}
$$

We can assume that $\exists\,\varepsilon > 0$, such that

$$
||f(\boldsymbol{p}(n+1),\lambda(n+1))||^2 < \varepsilon ||f(\boldsymbol{p}(n),\lambda(n))||^2. \tag{31}
$$

Then we have

$$
\lim_{n\to\infty} ||f(\boldsymbol{p}(n),\lambda(n))||^2 = 0. \tag{32}
$$

Therefore, a step length can be obtained during each iteration to achieve one equilibrium point of the system of differential Eq. (21). With Theorem 2, it is concluded that Algorithm 1 can converge to NE of the considered game.

5 Simulation results

5.1 Network parameters

Unless otherwise mentioned, the simulation is performed under the following network parameter settings. There are $N = 4$ SUs and $M = 3$ PUs in the network. The involved spectrum is divided into $K = 5$ channels and each channel has bandwidth $W = 1$ MHz. The SUs and PUs are randomly located in a $10\,\mathrm{m} \times 10\,\mathrm{m}$ square. Assume that path loss over channel k is in accordance with the classic path-loss model (Goldsmith, 2005), i.e.,

$$
L^k(d_{ij}) = L^k(d_0) + 10n\lg\left(\frac{d_{ij}}{d_0}\right),\ i \neq j, \tag{33}
$$

where the reference distance d_0 is set to 1 m, d_{ij} is the distance between SU_i-Tx and SU_j-Rx, and constant n is set to 4. The propagation loss in the free space is given by

$$
L^k(d_0) = \left(\frac{4\pi d_0}{\nu^k}\right)^2, \tag{34}
$$

where ν^k is the operating wavelength of channel k. Without loss of generality, the center frequency of the system is assumed to be 900 MHz. Thus, the power gain can be obtained as

$$
g_{ij}^k = \frac{1}{d_{ij}^4} \cdot \left(\frac{\nu^k d_0}{4\pi}\right)^2, \tag{35}
$$

$$
h_{im}^k = \frac{1}{d_{im}^4} \cdot \left(\frac{\nu^k d_0}{4\pi}\right)^2, \tag{36}
$$

where d_{im} is the distance between SU_i-Tx and PU_m. The background noise power is set to $10^{-8}\left|x_i^k\right|$, where x_i^k is subject to a random distribution in $[0, 1]$. The maximum possible transmit powers of SUs are set to 4, 3, 2, and 6 mW, respectively, and the interference power thresholds of PUs are set to 5×10^{-9}, 6×10^{-9}, and 4×10^{-9} W, respectively. Tolerable error ε is set to 10^{-8}.

5.2 Convergence and capacity analysis

Now we investigate the convergence and capacity of the proposed Algorithm 1. First, Fig. 2 shows the convergence of each SU's power strategy over each channel, from which we can observe that the transmit power evolves in a stepwise manner and the trends during the entire process may be inconsistent. After convergence, some SUs' total transmit power

will achieve the possible maximum total power. The interference created for PUs by SUs is illustrated in Fig. 3. As shown in Fig. 3, the interference to each PU increases all along, and some PUs' interference power thresholds are reached. Figs. 2 and 3 demonstrate that the power strategy satisfies all the constraints imposed after convergence.
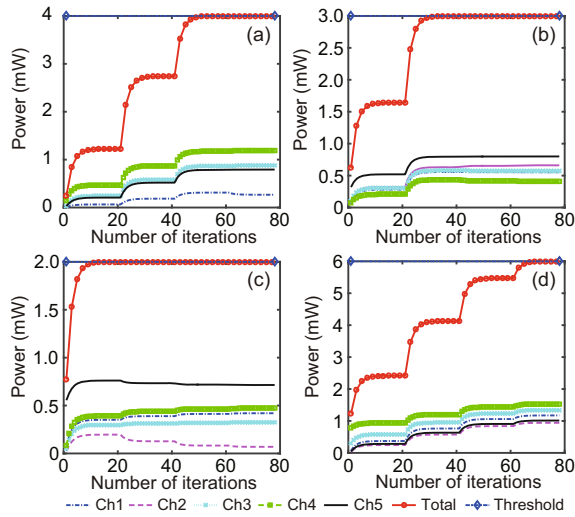

Fig. 2 Convergence of four SUs' power strategy over five channels: (a) SU1; (b) SU2; (c) SU3; (d) SU4 (SU: secondary user)
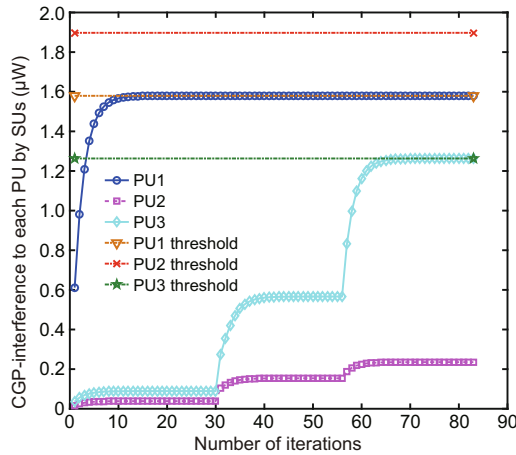

Fig. 3 Convergence of interference created for PUs by SUs

PU: primary user; SU: secondary user; CGP: centralized gradient projection

Fig. 4 shows the convergence of each SU's rate and the whole secondary system's throughput. Similarly, the channel throughput evolves in a stepwise manner and the trends during the entire process may be inconsistent. Channel capacity versus different

maximum possible transmit power is illustrated in Fig. 5. We change only the maximum possible transmit power of SU4 while holding the other three SUs' maximum possible transmit power constant. It can be seen that the channel capacity of SU4 improves along with the increase of its maximum transmit power, while other SUs' capacities slightly decrease. Also, we can see that the total secondary capacity shows a little improvement as the whole maximum possible transmit power increases.

5.3 Effectiveness analysis

To verify the effectiveness of the proposed CGP algorithm, we compare it with the distributed multichannel power allocation (DMPA) algorithm using the Lagrange dual decomposition in Wu and Tsang (2008). The DMPA algorithm requires that the link
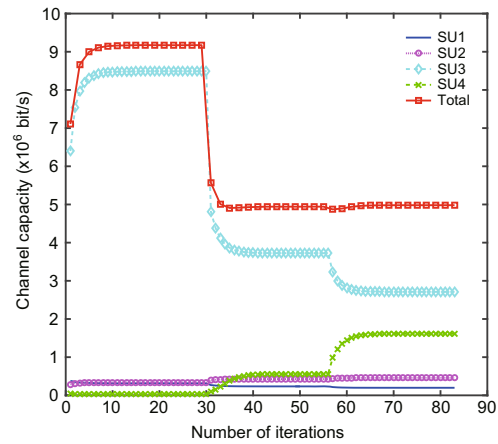
Fig. 4 Rate convergence of each SU and the throughput of the whole secondary system (SU: secondary user)
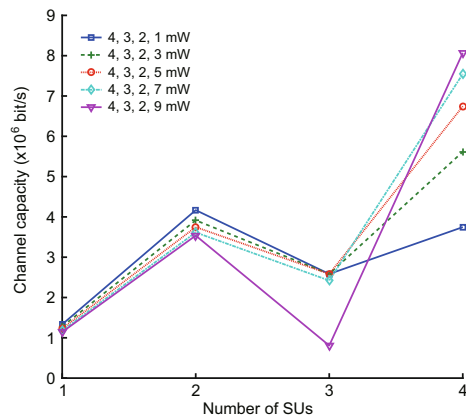
Fig. 5 Channel capacity versus different maximum possible transmit power (SU: secondary user)

power gain among SUs satisfy an assumption

$$
\begin{cases}
(g_{ii}^k)^2 \geq \sum\limits_{\substack{j=1 \\ j \neq i}}^{N} g_{ii}^k g_{ji}^k, \\
(g_{ii}^k)^2 \geq \sum\limits_{\substack{j=1 \\ j \neq i}}^{N} g_{jj}^k g_{ij}^k,
\end{cases}
\text{where}
\begin{cases}
i = 1, 2, \cdots, N, \\
k = 1, 2, \cdots, K,
\end{cases}
$$
(37)

i.e., relatively low level interference among SUs (or high SINR). Thus, g_{ij}^k $(j \neq i)$ is kept unchanged and g_{ii}^k is set to satisfy constraint (37), which guarantees the uniqueness of the NE of G by Wu and Tsang (2008). Other parameters are kept the same to guarantee a fair comparison.

Table 1 shows the performance comparison of the two algorithms in terms of a power strategy of four SUs over five channels, the channel throughput of each SU, and the interference suffered from three PUs. Within error tolerance, it can be concluded that the two algorithms converge to the same power strategy, and the channel throughput of each SU and the interference suffered from PUs are the same as well. Comparison of the two algorithms in terms of the interference created for PUs is shown in Figs. 6 and 7. From Fig. 6, it can be observed that the interference created for PUs by SUs continues to increase when some PUs' interference threshold is exceeded and converges at the threshold exceeded for a period of time. However, for the CGP algorithm (Fig. 7), interference suffered from PUs increases all along during the procedure and never exceeds any PU's interference threshold. Furthermore, the interference does not exhibit a process of first rising and then declining, reflecting the good effectiveness of the CGP algorithm.

It can be concluded that although the two algorithms achieve a similar power strategy, secondary throughput, and interference level, CGP has a much
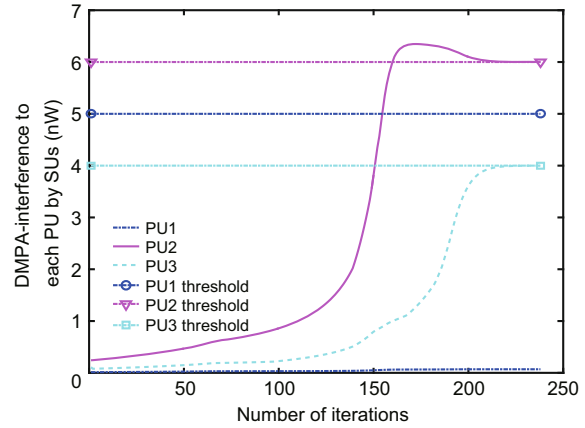
Fig. 6 DMPA convergence of interference created for PUs by SUs
DMPA: distributed multichannel power allocation; PU: primary user; SU: secondary user
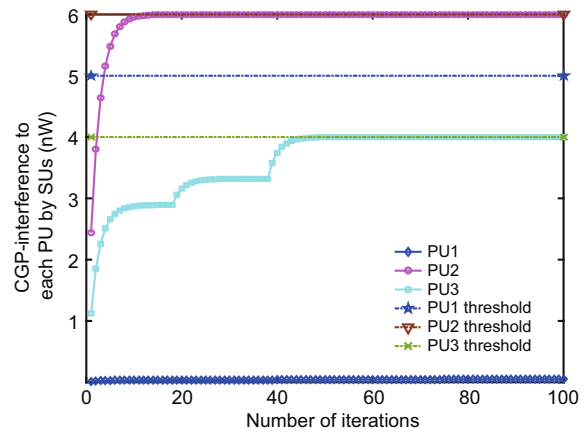

Fig. 7 CGP convergence of interference created for PUs by SUs
CGP: centralized gradient projection; PU: primary user; SU: secondary user

Table 1 Comparison of distributed multichannel power allocation (DMPA) and centralized gradient projection (CGP)

Algorithm	Power (W)					Capacity (Mb/s)				Interference (nW)		
	SU1	SU2	SU3	SU4	SU5	SU1	SU2	SU3	SU4	SU1	SU2	SU3
DPMA	0	0.1144	0.1267	0.5329	0	2.4260	2.9980	6.7620	12.7530	3.9470	6.0000	0.2960
	0.4736	0.8099	0.5063	0.4188	0.7892							
	0.4332	0.0241	0.3348	0.5029	0.7047							
	1.2251	0.9404	1.4053	1.3618	1.0658							
CGP	0	0.1451	0.0950	0.5337	0	2.4230	2.9980	6.7630	12.8280	3.9480	6.0000	0.2960
	0.4740	0.8109	0.5062	0.4192	0.7896							
	0.4333	0.0281	0.3307	0.5032	0.7047							
	1.2254	0.9425	1.4037	1.3623	1.0661							

higher convergence speed and is more stable, compared with the DMPA algorithm. Moreover, DMPA demands a relatively high SINR of SUs, without which it is not able to converge. Thus, we can conclude from constraint (37) that it is not always met in practice. Conversely, the CGP algorithm can be implemented regardless of the power gain among SUs, revealing good effectiveness and a broad channel condition applicability.

5.4 Robustness analysis

To test and verify the robustness of our proposed algorithm, we further study the impact of network scale characterized by the number of SUs. To control variables as much as possible, thus ensuring a fair comparison, the proposed network scenario is determined as follows: consider the same network parameters as depicted in Section 5.1. The number, location, and interference power constraints of PUs are unchanged. As for the CR network, using the four-pair CR network considered above as a model, keeping the topology location, background noise power, and maximum transmit power constraints of SUs unchanged, and by scaling down the model area by a ratio of n, we introduce $4n$ SU transceivers to the network. The network scenario is illustrated in Fig. 8 for the case of $n = 3$. Each simulation round randomly generates a CR network topology model, and the average results of 1000 simulation rounds are shown in Figs. 9 and 10.

Fig. 9 shows the required number of iterations of CGP vs. the number of SUs. It is shown that, with the growth in the number of SUs, the required number of iterations increases first, reaching a peak with 24 SUs, and then decreases. Fig. 10 shows the running time of CGP vs. the number of SUs; note that the curve shows a trend different from that in Fig. 9. When the number of SUs is less than 28, the running time increases rapidly; when the number of SUs is larger than 28, the running time fluctuates around 1 s. Compared with Fig. 9, it can be extrapolated that, when the number of SUs is larger than 28, with the increase in the number of SUs, the average time consumed during each iteration increases. However, Figs. 9 and 10 indicate that implementing the proposed algorithm, the delay involved in the central control node which sends the power allocation policy is tolerable when the network scale expands, reflecting the good robustness of the CGP algorithm.
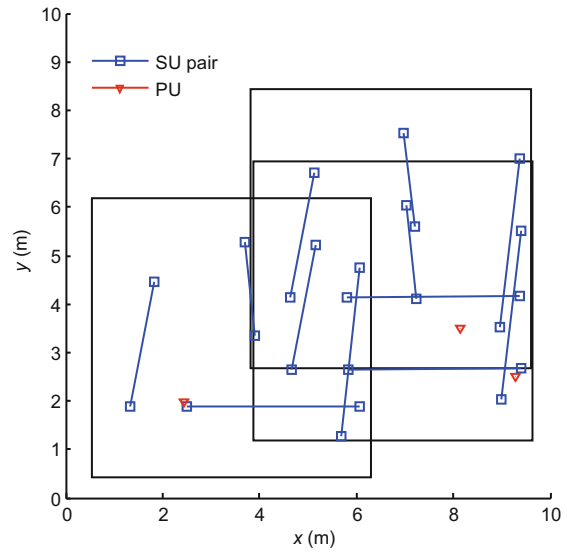

Fig. 8   Location of SUs and PUs in the network
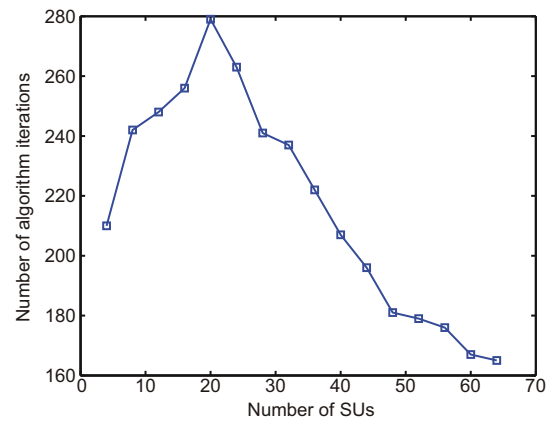
PU: primary user; SU: secondary user

Fig. 9   Required number of iterations vs. number of SUs (SU: secondary user)
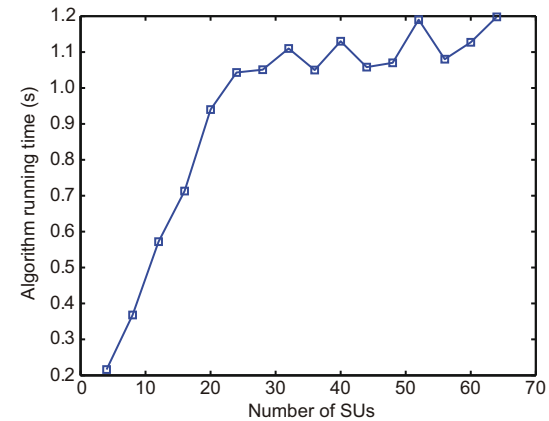

Fig. 10   Running time vs. number of SUs (SU: secondary user)

6 Conclusions and future work

In this paper, we have studied the important power control problem for SUs in a CR network with multiple PUs and multiple channels. We have formulated the power control problem as a non-cooperative game with coupled constraints. Due to the complexity of finding the NE of the original game, we have proposed a projected gradient based dynamic model and converted the problem into finding the equilibrium points of the proposed model. Then we have derived a centralized algorithm to solve the problem. Through simulation results, we showed that our proposed algorithm is robust, and that its convergence and effectiveness are competitive.

The power control scheme demonstrated in this paper is centralized, which may not be suitable for fast time-varying channels. Therefore, our future work will focus on implementing the proposed scheme in a distributed manner. Moreover, during the process of solving the problem, we observed that there exists more than one NE in the original game. Therefore, the optimality analysis of the proposed solution is also an interesting and challenging problem.

References

Arrow K, Hurwicz L, Uzawa H, 1961. Constraint qualifications in maximization problems. *Nav Res Log Q*, 8(2):175-191. https://doi.org/10.1002/nav.3800080206

Bedeer E, Dobre O, Ahmed M, et al., 2014. A multiobjective optimization approach for optimal link adaptation of OFDM-based cognitive radio systems with imperfect spectrum sensing. *IEEE Trans Wirel Commun*, 13(4):2339-2351.
https://doi.org/10.1109/TWC.2014.022114.131948

Goldsmith A, 2005. Wireless Communications. Cambridge University Press, Cambridge, UK.

Han Z, Niyato D, Basar T, et al., 2012. Game Theory in Wireless and Communication Networks. Cambridge University Press, Cambridge, UK.

Kolodzy P, 2006. Interference temperature: a metric for dynamic spectrum utilization. *Int J Netw Manag*, 16(2):103-113. https://doi.org/10.1002/nem.608

Le LB, Hossain E, 2008. Resource allocation for spectrum underlay in cognitive radio networks. *IEEE Trans Wirel Commun*, 7(12):5306-5315.
https://doi.org/10.1109/T-WC.2008.070890

Lin Y, Liu K, Hsieh H, 2010. Design of power control protocols for spectrum sharing in cognitive radio networks: a game-theoretic perspective. IEEE Int Conf on Communications, p.1-6.
https://doi.org/10.1109/ICC.2010.5502441

Mercier B, Fodor V, Thobaben R, et al., 2008. Sensor networks for cognitive radio: theory and system design. Proc ICT Mobile and Wireless Communications Summit, p.10-17.
https://doi.org/10.1109/ICECTECH.2011.5941743

Neel J, Reed J, Gilles R, 2004. Convergence of cognitive radio networks. IEEE Wirel Communication and Networking Conf, p.2250-2255.
https://doi.org/10.1109/WCNC.2004.1311438

Rosen J, 1960. The gradient projection method for nonlinear programming. Part I. Linear constraints. *J Soc Ind Appl Math*, 8(1):181-217.
https://doi.org/10.1137/0108011

Rosen J, 1965. Existence and uniqueness of equilibrium points for concave n-person games. *Econometrica*, 33(3):520-534. https://doi.org/10.2307/1911749

Wang Z, Jiang L, He C, 2013. A novel price-based power control algorithm in cognitive radio networks. *IEEE Commun Lett*, 17(1):43-46.
https://doi.org/10.1109/LCOMM.2012.120612.121587

Wild B, Ramchandran K, 2005. Detecting primary receivers for cognitive radio applications. 1st IEEE Int Symp on New Frontiers in Dynamic Spectrum Access Networks, p.124-130.
https://doi.org/10.1109/DYSPAN.2005.1542626

Wu Y, Tsang D, 2008. Distributed multichannel power allocation algorithm for spectrum sharing cognitive radio networks. IEEE Wireless Communications and Networking Conf, p.1436-1441.
https://doi.org/10.1109/WCNC.2008.258

Yang G, Li B, Tan X, et al., 2015. Adaptive power control algorithm in cognitive radio based on game theory. *IET Commun*, 9(15):1807-1811.
https://doi.org/10.1049/iet-com.2014.1109

Zhou P, Chang Y, Copeland J, 2012. Reinforcement learning for repeated power control game in cognitive radio networks. *IEEE J Sel Areas Commun*, 30(1):54-69.
https://doi.org/10.1109/JSAC.2012.120106